20th Annual Conference of the Canadian Nuclear Society
Montreal, Quebec, Canada / May 30 - June 2, 1999

Computer Simulation of Aerosol Dynamics With A Unified Agglomeration Kernel

Yves B. Trudeau[1], Wen Chao Chen[1] C. Keith Scott[2], and Kenneth Oxorn[1]

[1] *ANIQ R&D Inc., Laboratoire René-J.-A.-Lévesque, Université de Montréal, C.P. 6128, succursale Centre–ville, Montréal, Québec H3C 3J7*

[2] *Atlantic Nuclear Services Ltd., P.O. Box 1268, Fredericton, N. B. E3B 5C8*

Abstract

Aerosol dynamics have been simulated with the computer code CONTAIN using a modified agglomeration kernel. The time (t) evolution of the size distribution ($n_k(t)$) and the suspended mass concentration of particles of size index k was calculated for both the new kernel and the standard superposition kernel. In addition, the fractal nature of the particle geometry has been accounted for and the implications on the distributions are discussed.

1 Introduction

The CONTAIN code, for simulating the containment response to severe core accidents, has been used to investigate different models of aerosol dynamics. CONTAIN is particularly well suited as a test-bench because it integrates the models that describe the various phenomena that occur in the containment. There is indeed a high level of interaction between aerosol dynamics and thermal hydraulics conditions. Hence a very accurate aerosol model is desirable, not only because the most significant releases of radioactive material typically occur via aerosol escape, but also because aerosol dynamics would affect the thermal–hydraulics parameters which determine whether or not the integrity of the containment is breached [1].

During a severe core accident, aerosol particles may be released from the reactor vessel into the containment volume, where they will remain for some time, collide with each other and agglomerate, hit the walls and deposit there, fall to the floor, fragment under the influence of atmospheric turbulence, be collected by water drops from the sprays and have water condense on or evaporate from their surface. These aerosol processes depend on the particle size, which typically varies from 0.01 to 10 μm, so the evolution of aerosol particle size distributions is at the center of the aerosol dynamics model.

When two particles collide, they agglomerate and form a larger one. The kernel is the probability per unit time for two particles to collide. In the CONTAIN 2.0 distribution, as with most codes that calculate aerosol dynamics, the aerosol model assumes that collisions occur either under the effect of gravitational force, Brownian motion, or turbulence (both diffusional and inertial). A kernel is calculated independently for each of these effects and all the kernels are algebraically summed afterward. Physically, collisions between particles occur because of diffusion or because they have acquired a relative velocity and the collisions should be treated as concurrent processes. Therefore we propose to replace the superposition kernel with the new unified kernel based on the relative velocity and the diffusion coefficient of the particles.

In this contribution, the kernels and the suspended mass concentration were calculated using either the superposition of single process kernels or the new "unified" kernel. Both results are compared and discussed. In addition, the proposed collision kernel accounts for the fractal nature of the particles. The model's adjustable parameters are identified and their influence on the kernels and the mass concentrations is discussed. The influence of fragmentation on the suspended mass concentration is a relevant but complex problem that will be investigated at a later date. The results from the first phase of this study are presented. The summation kernel originaly used in CONTAIN and the unified kernel are plotted for comparison and their effect is observed on the particle size distributions during a simulated aerosol dynamics experiment.

2 Physical Model

When studying aerosol dynamics in the containment, after a breach in the reactor vessel, one has to consider the agglomeration and the removal of the particles under the influence of Brownian motion, gravitational acceleration,

turbulence, source injection, condensation/evaporation of water on the particles, the properties of each chemical component (such as the activity of certain isotopes and hygroscopicity), as well as the interaction between the aerosols and thermal hydraulics parameters. The quantities of interest are the particle size distribution ($n_k(t)$) and the suspended mass concentration ($n_k(t)m_k$) for a particle of size class k. The agglomeration mechanisms are usually represented by the collision kernel K_{ij}, which gives the collision rate between a particle of size class i and a particle of size class j. Agglomeration is assumed to proceed from the collision of only two particles. The particle size evolution is governed by the generalized Smoluchowski equation, which is written as:

$$\begin{aligned}\frac{\partial n_k(t)}{\partial t} &= \frac{1}{2}\sum_{i+j=k} K_{ij} n_i(t) n_j(t) - \sum_j K_{kj} n_k(t) n_j(t) \\ &\quad + S_k(t) - R_k(t) n_k(t) - \frac{\partial (I_k(t) n_k(t))}{\partial k}\,. \end{aligned} \tag{1}$$

The first summation on the right hand side of the equation represents the agglomeration of a particle of size class i with a particle of size class j, to form a particle of size class k. The second sum on the right hand side of the equation represents the depletion in population of size class k, due to the agglomeration of these particles with particles of size class j. S_k is the source term for aerosols released into the containment. R_k represents the removal processes, and finally, the last term represents water condensation on or evaporation from the particle surface.

With the proposed model, K_{ij} is a single kernel which combines the effect of Brownian motion, the gravitational force and the turbulence effects, expressed with the mean relative velocity. For simplicity, we replace the index i by the corresponding radius, which we write as a, and the index j by its corresponding radius, b. The calculated kernel is given by [2]:

$$K(a,b) = \frac{\pi (a+b)^2 V}{G(\chi,\beta)} \tag{2}$$

where

$$G(\chi,\beta) = 1 - 2\exp\left(\frac{\beta}{4\chi}\tan^{-1}(\chi)\right) \times \int_1^\infty \frac{dy}{y^3}\exp\left(-\frac{\beta}{4\chi}\tan^{-1}(\chi y)\right) \tag{3}$$

with

$$\chi = (a+b)\left(\frac{k_e}{D_B}\right)^{1/2}\,, \tag{4}$$

and

$$\beta = \frac{(a+b)V}{D_B}\,. \tag{5}$$

Hence β measures the ratio of the inertial effect to the Brownian effect, while χ^2 gives the ratio of the local turbulence effect to the Brownian effect. The net relative velocity [3] V is given by

$$V = \epsilon(a,b)\,|\tau_a - \tau_b|\,\sqrt{3.9\frac{\varepsilon_T^{3/2}}{\nu^{1/2}} + g^2}\,, \tag{6}$$

where τ_a and τ_b are the relaxation times, or characteristic times, for particle a and particle b respectively, g the gravitational acceleration, ν the kinematic viscosity, and ε_T the turbulence energy dissipation rate. Originally [2] the collision efficiency $\epsilon(a,b)$ was not discussed, and we have inserted it here with the relative velocity, where it applies equally to the gravitational and turbulent inertial effects while leaving the diffusional processes unaffected, as most authors do when working with individually calculated kernels. The collision efficiency will be discussed further below.

In Eq. (4), $k_e = \beta_0\,(\varepsilon_T/\nu)^{1/2}$ with $\beta_0 = 0.15$ and $D_B = D_a + D_b$. D_a and D_b are the diffusion coefficients for particles a and b respectively. The relaxation time is written as

$$\tau_a = \frac{2\rho C(a) a^2}{9\eta\kappa}\,. \tag{7}$$

where κ is the dynamic shape factor (κ is introduced in the calculation of the frictional drag force when the Stokes-Einstein law is assumed to still be valid for non–spherical particles), η the carrier gas viscosity, and $C(a)$ the Cunningham slip flow correction factor, defined as usual:

$$C(a) = 1 + 1.246K_n + 0.42K_n\exp(-0.87/K_n)\,. \tag{8}$$

Here, K_n is the Knudsen number and is defined as $K_n = \lambda/a$, where λ is the mean free path length of the carrier gas. It should be noted that the integral in Eq. (3) has no analytical solution and should be solved numerically.

When the cluster is a fractal particle, its size is given by its effective radius a_{eff} (sometimes also called geometrical radius) [7]:

$$a_{eff} = R_0\left(\frac{v_a}{v_0}\right)^{1/d_f}\,. \tag{9}$$

In Eq. (9), d_f is the fractal dimension which is obtained from experiments, R_0 and v_0 are the radius and volume of the elemental spherules the particle is made of, and v_a is the occupied volume in the cluster. In order to include the fractal description in the collision kernel, a is replaced by a_{eff} in the diffusion coefficient D_B, the relative velocity V and Eqs. (2,4—8).

3 The CONTAIN Aerosol Module

This section describes the computational methods and the modifications made to the aerosol module of CONTAIN in order to include the new unified kernel for fractal particles.

3.1 Computational methods

Eqs. (1) and (2) have no analytical solution. The numerical calculation of Eq. (1) is usually based on the Runge-Kutta-Merson method, but this method requires significant computational power and it presents instabilities when the equation is stated as above. However, these problems have been overcome by making use of the sectional method proposed by Gelbard et al. [4], for single component aerosols, and Gelbard and Seinfeld [5] for multiple components. Since the multicomponent method has already been implemented in CONTAIN, we elected to use the Gelbard and Seinfeld method for solving Eq. (1).

In order to calculate numerically the unified kernel, it is important to select an appropriate numerical method to evaluate the semi–infinite integral in Eq. (3). For this purpose, the method of integration proposed by Piessens and de Doncker [6] has been found helpful.

The aerosol dynamics equation depends on a number of variables $(T, g, \epsilon_T, \eta, v_0, t)$, which can be measured or controlled experimentally, and adjustable parameters $(\kappa, \epsilon(a,b), \beta_0, \lambda)$ that can be extracted from experimental data.

4 Results

Fig. 1 shows a comparison between the unified model and the superposition model of the agglomeration kernel as a function of the radius of particle b. Eq. (2) was used to calculate the unified kernel (K_{Tot}) and the usual CONTAIN aerosol model for the calculation of the superposition kernel ($K_B + K_G + K_T$). The test particle size was $a = 1\,\mu$m and the gas temperature $T = 373$ K. Fig. 1 also shows the individual kernel contributions: Brownian motion (K_B), gravitational force (K_G) and turbulence (K_T), as indicated within the figure.

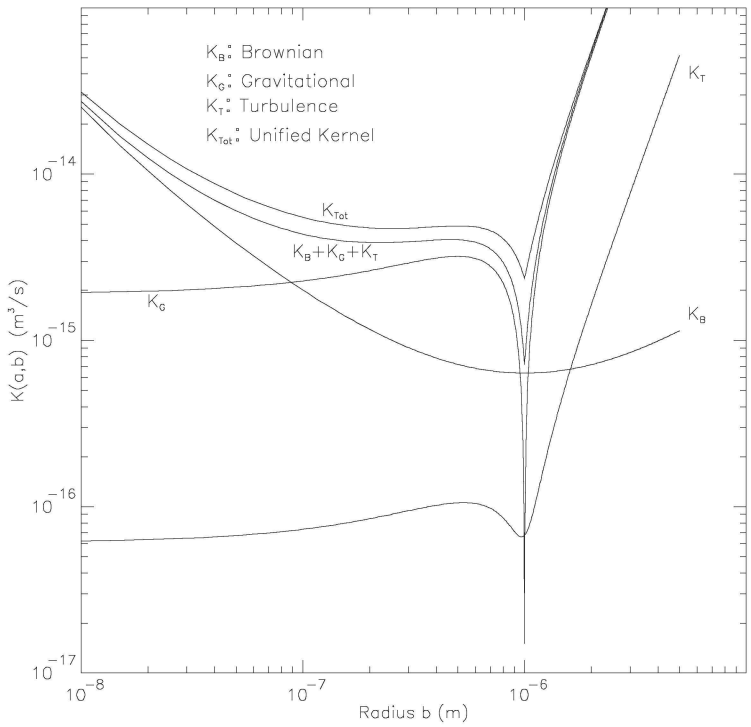

Figure 1: Comparison of the agglomeration kernels at $T = 373$ K, $a = 1\mu$m and $\epsilon(a, b) = 1$. K_{tot}, K_B, K_G and K_T represent the calculation for the unified, Brownian, gravitational and turbulence kernels respectively.

The fractal structure also has an important influence on particle agglomeration. This effect is shown in Fig. 2 for the superposition kernel and in Fig. 3 for

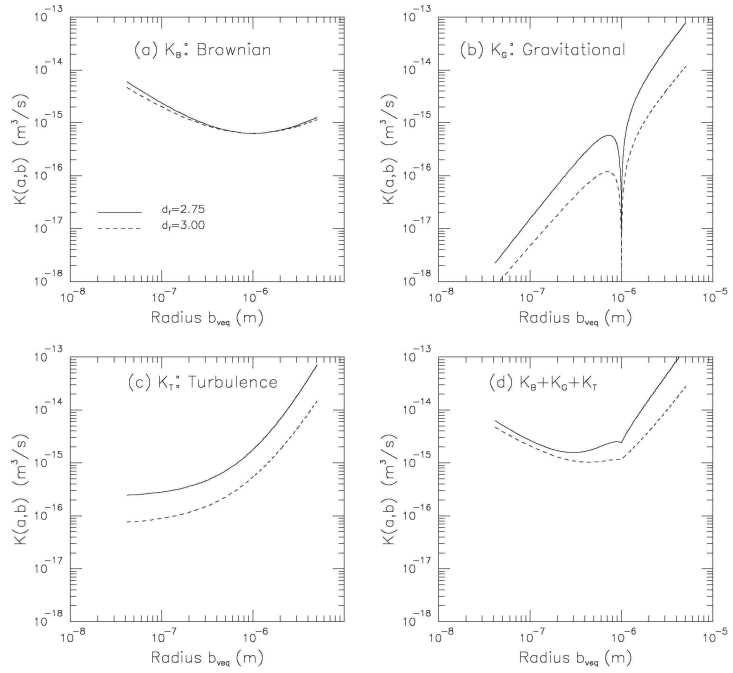

Figure 2: Comparison of the agglomeration kernels at $T = 373$ K for a test particle of radius $a = 1\mu$m. K_B, K_G and K_T represent the calculation for the Brownian, gravitational, turbulence kernels. The solid and the dashed curves are calculated with $d_f = 2.75$ and $d_f = 3.00$ (spherical particles) respectively. The collision efficiency is given by Eq. (10).

the unified kernel. In Fig. 2, the superposition kernel is displayed for a fractal dimension $d_f = 3.0$, as well as for $d_f = 2.75$, which corresponds to the fractal dimension previously measured on silica particle clusters [9]. The Brownian, gravitational and turbulence contributions are shown in Fig. 2 (a), (b) and (c) respectively. The summation kernel is shown in Fig. 2. In Fig. 3, the unified kernel with $d_f = 2.75$ is compared with the unified kernel for $d_f = 3.0$, as a function of the effective (geometrical) radius b.

The following discussion is based on the mass concentration results which represent the number of particles having a mass that corresponds to the size class k. A standard CONTAIN input file was used for testing the aerosol

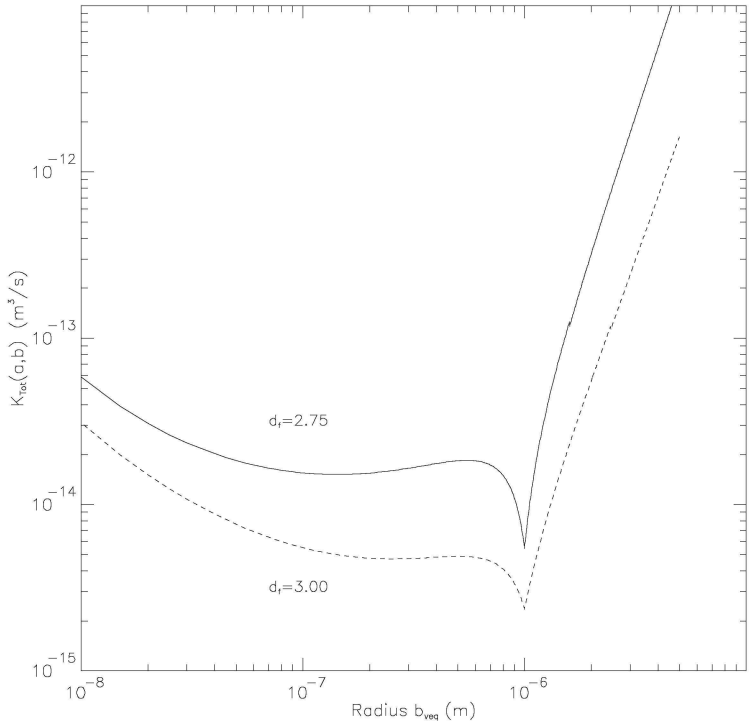

Figure 3: Comparison of the unified kernel for $d_f = 3.00$ (no fractals) with $d_f = 2.75$ (with fractals) at $T = 373$ K, with $a = 1\mu$m and $\epsilon = 1$.

model, namely the 5–cell Surtsey deck for experiment IET-3, rev.2 supplied with the CONTAIN 2.0 code. The default parameters were used except for those specified in the figures, and water condensation on or evaporation from the aerosol particles was turned off for simplicity, but all the other models in CONTAIN were active. The results of a calculation of the suspended mass concentration as a function of the particle diameter is shown in Fig. 4 for a simple case where there is no condensation/evaporation, and no source term in the Smoluchowski equation. The mass concentration is calculated at $t = 0$, 2.2, 3, 4, 7, and 15 s in a containment structure consisting of 4 different cells, as indicated in Fig. 4. This run was initiated with a total suspended mass of 2 kg of *Fe* in cell no 1. The initial total mass concentration is calculated to be $5.54\,\mathrm{kg/m^3}$ in cell 1 and 0 for the other cells. The initial concentration is

shown in Fig. 4 with filled circles connected by continuous lines. For $t > 0$, the inter-cell transport takes effect, and the mass concentration in cells 2, 3, 4 and 5 increases. The result is shown in Figs. 4 (b), (c) and (d) with the solid, dashed, dotted, and dashed-dotted lines corresponding to increasing specified times after the injection of aerosols in cell 1. It should be noted that, due to the deposition of particles on the roofs, walls, pools and floors, the total suspended particle mass is not 2 kg but the sum of suspended and deposited masses gives effectively 2 kg. Table 1 shows the details of the suspended total mass and the deposited total mass at $t = 3$ s. This result shows that there is conservation of the mass throughout the system. The same calculations were performed with the summation kernel and they led to results (not shown) that do not significantly differ from those obtained with the unified kernel.

Cell no	1	2	3	4	5
Suspended total mass (kg)	0.3588	0.01764	0.03243	0.7403	0.8088
Deposited total mass (kg)	0.0	0.0	0.01281	0.02738	0.001831

Table 1: Details of the suspended and deposited total mass for different cells at $t = 3$ s.

5 Discussion

When particle collisions are treated ballistically, as a first step in the calculation of a collision kernel, the effect of the fluid on the movement of the particles is not yet considered. To do so one introduces the collision efficiency factor. The impact of this multiplicative factor on the kernel is especially significant when the size of the colliding particles is quite different. For instance, when a small particle heads towards a much larger test–particle, there is a high probability that it will be deflected off its original course, follow the fluid flow lines around the large particle and avoid the collision altogether. Several mathematical expressions have been suggested for the collision efficiency; the following equation has been used in the calculations presented here and it is known to agree reasonably well with experimental data.[10]

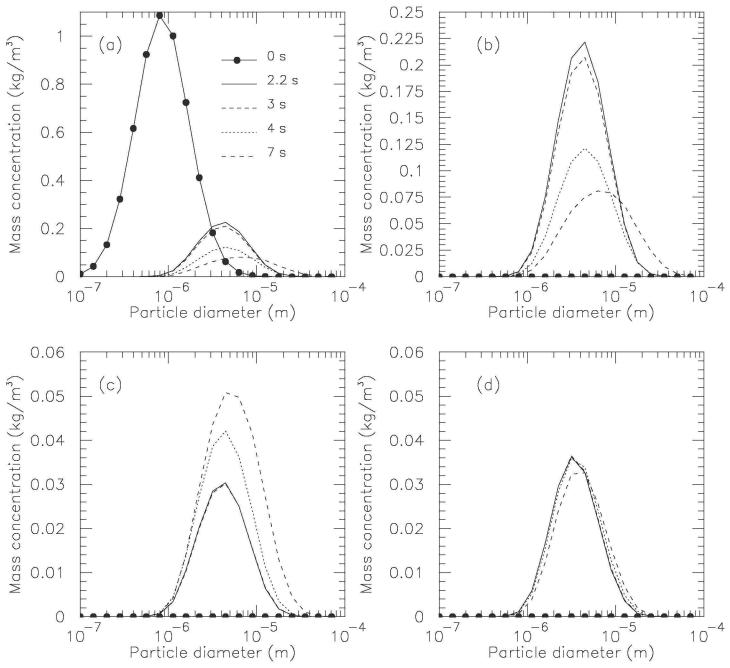

Figure 4: Suspended mass concentration in different cells as a function of the particle diameter. Each line corresponds to a different agglomeration time, as indicated in the figure. The initial total mass of *Fe* was 2 kg, corresponding to a mass concentration of $5.54\,\mathrm{kg/m^3}$. The calculations were made with the unified kernel for hard spherical particles and $\varepsilon_T = 10^{-3}\ \mathrm{m^2/s^3}$

$$\epsilon(a,b) = 1.5(c/(a+b))^2\,, \tag{10}$$

where c is the smaller of a and b.

The increase in the value of the collision kernel when the fractal dimension is reduced from 3.0 to 2.75 was an expected feature of Figs. 2 and 3. A particle that has a more open structure (lower fractal dimension) will extend over a larger volume than a more compact particle of the same mass made from the same elements. In other words, the particle of low fractal dimension will have a larger cross section and will have a higher probability of colliding with other particles than a compact particle of the same volume–equivalent dimension. A

similar trend has been observed elsewhere [12], but it has proved difficult to establish quantitative comparisons with our work, presumably because not all of the input parameters have been supplied.

In Fig. 2, where the collision efficiency is given by Eq. (10), the Brownian motion and the gravitational force effects are dominant for small and large particles respectively, as expected. In the region where $a \simeq b$, the turbulent aggregation can be more important than other aggregation mechanisms, depending on the turbulent energy deposition rate (here $\varepsilon_T = 10^{-3}$ m^2/s^3). The unified kernel in Fig. 1 is always distinctly greater than the summation kernel. When Eq. (10) is used, the gravitational and the turbulence kernels are decreased for small particles (See Figs. 1 and 2).

For the unified kernel, it is possible to test numerically the limiting cases. The results of the test are shown in Table 2 for three different special cases. The Brownian plus gravitational kernel is found when $\beta \to 0$ and $a \approx b$. In particular, the Brownian kernel itself is obtained when $\chi \leq 10^{-5}$. In addition, the unified kernel reduces to the gravitational plus turbulence kernel when $\beta \to \infty$ and $\chi \to 0$ (The actual values used for the numerical calculation are shown in the table). It is easy to show that the analytical expression for the special case $\beta \to \infty$, $\chi \to 0$ and $G(\chi, \beta) = 1$ is:

$$K_{GT}(a, b) = K(a, b) = \pi(a + b)^2 V \, . \tag{11}$$

This equation agrees with our numerical calculations. These verifications give more confidence in the numerical evaluation of the unified kernel. It is clear that the differences between K_{tot} and K_{sum} shown in Figs. 1 and 2 should affect the particle distribution $n(a, t)$.

Case	Values used	Explicit sum	Tested
$\beta \to 0$	$dx \approx dy$	B + G	$\surd$
$\beta \to 0$	$dx \approx dy$ $\quad \chi \leq 10^{-5}$	B	$\surd$
$\beta \to \infty$	$\beta \geq 10^3$ $\quad \chi = 10^{-15}$	G + T	$\surd$

Table 2: Testing of the limit cases of the new agglomeration kernel. The mathematical expressions of the unified kernel limit cases are given in [2].

The effect of the collision efficiency on the mass concentration is shown in Fig. 5. Clearly, for particle of size between 10^{-6} and 10^{-5} m, the mass concentration is enhanced when Eq. (10) is used for the collision efficiency instead of $\epsilon(a, b) =$

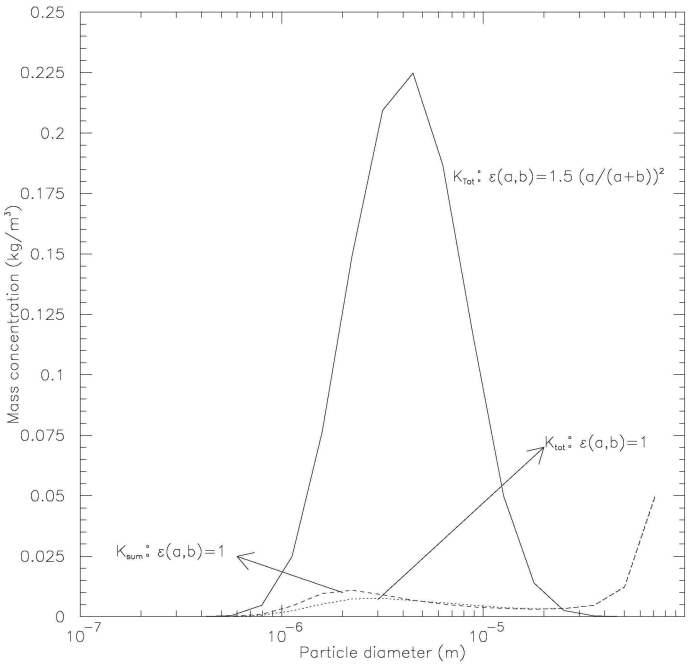

Figure 5: Effect of the collision efficiency on the mass concentration. The solid and dotted lines represent the unified kernel calculation for $\epsilon(a,b) = 1.5(a/(a+b))^2$ where $a < b$, and $\epsilon(a,b) = 1$, respectively. The dashed line represent the superposition kernel calculation for $\epsilon(a,b) = 1$.

1 (dotted curve). The mass concentration for the summation kernel K_{sum} is also shown in Fig. 5. In general, the value of ϵ is smaller than 1. This implies that the the value of β is much smaller and $G(\chi,\beta) < 1$. Therefore, the total kernel in Eq. (2) is enhanced. Without the collision efficiency, extremely large particles will be formed as shown in Fig. 5. This result will depart from the experimental data.

6 Conclusion

The calculation of the kernels has shown that the superposition kernel falls short of the more realistic unified kernel. For the test case reported here

turbulent agglomeration contributes little. Therfore we expect the two representations to be very close. This discrepancy will be the subject of further investigation.

The inclusion of a fractal dimension of 2.75 in the unified kernel increases the value of the kernel by approximately one order of magnitude. Based on the results presented here and another report in the literature,[8] an explicit account of the fractal dimension of the particles leads to a much larger collision kernel that promotes the formation of very large particles and the model is not expected to be representative unless fragmentation is included at the same time.

Our results have shown that it is just as important to include a proper collision efficiency factor in the unified kernel as it is with the usual summation kernel. We believe that the unified kernel is more appropriate than the sum of independently calculated single–effect kernels, that it will prove to be more accurate and that it will increase the predictive capacity of aerosol dynamics modelling in more complex scenarios. Also, the representation of the kernel requires fewer empirical parameters to define the process.

6.1 Extension to accident sequence and further developments

This investigation of the aerosol dynamics will be pursued along three lines. Firstly, the sensitivity of the kernel and the suspended mass distributions to parameters such as the aerosol material density and the turbulent energy dissipation will be assessed. The unified kernel of Eq. (1) will also be tested on a timescale and under conditions that are more representative of an accident scenario and the results will be compared to those obtained with the summation kernel. Secondly, fragmentation will be modelled and tests will be run on the effect of fragmentation and the fractal dimension of the particles. Thirdly, the relative velocity of the particles with respect to the fluid will be taken into account. The last two items are discussed below.

According to the present models (both unified and summation kernels), once a particle starts to agglomerate there is nothing to stop it from growing to an unrealistic size. The particles are exposed to external forces that can break a bond between the smallest constituents and split the particles into smaller particles. This process of fragmentation, when inserted in the Smoluchowski

equation, changes the structure of the equation and significantly complicates it. Although fragmentation is observed experimentally in the presence of turbulence [9], under some circumstances it may not be essential to account for fragmentation. For instance, fragmentation is less important if the agglomeration time is short, or if the large simulated particles settle before they reach unstable proportions.

The problem of the vectorial aspect of the particles' relative velocity will be addressed in the last phase of the project. The relative velocity expressed in Eq. (6) is effectively based on a statistical argument by Saffmann and Turner [3] that allows one to work with a scalar relative velocity. But a real particle is submitted to the concurrent effects of gravitation and fluid flow. For example, if the flow happens to be upward the velocity acquired by the particle will be less than either the gravitational velocity or the fluid flow velocity calculated independently. To avoid this problem the model should use a vectorial velocity, which leads to a diffusion equation that is more complexe and kernel calculations that are more involved [2].

Acknowledgements

We would like to thank the U.S. Nuclear Regulatory Commission and Sandia National Laboratory for allowing us to use the CONTAIN 2.0 code. This work was supported by the Microgravity Science Program of the Canadian Space Agency.

References

[1] Williams D.C., Bergeron K.D., Rexroth P.E., Tills J.L.; "Integrated phenomenological analysis of containment response to severe core damage accidents", *Prog. in Nuclear Energy* **19** (1987) 69.

[2] Williams M.M.R.; *"A unified theory of aerosol coagulation", J. Phys.* **D21** (1988) 875.

[3] Saffman, P.G. and Turner, J.S., *"On the Collision of Drops in Turbulent Clouds", J. Fluid Mech.*, **1**, (1956) 16.

[4] Gelbard F, Tambour Y, Seinfeld J.H.; "Sectional representations for simulaing aerosol dynamics", *Journal of Colloid and Interface Science* **76** (1980) 541.

[5] Gelbard F, Seinfeld J.H.; "Simulation of multicomponent aerosol dynamics", *Journal of Colloid and Interface Science* **78** (1980) 485.

[6] Piessens R. and de Doncker E., The integration fonction could be found at www.netlib.org/quadpack/dqagi.f, 1983.

[7] Simons S.; *"The effect of coagulation on steady–state Brownian diffusion of particles with a fractal structure", J. Phys.* **D20** (1987) 1197.

[8] Simons S., Simpson D.R.; *Ann. nucl. Energy* **16** (1989) 357.

[9] Scott C. K., Abdelbaky M.; to be published.

[10] Gelbard F., Aerosol Science and Technology, Vol. 12, p. 399, 1990.

[11] Murata K.K., Williams D.C., Tills J., Griffith R.O., Gido R.G., Tadios E.L., Davis F.J., Martinez G.M., Washington K.E.; "Code Manual for CONTAIN 2.0: A Computer Code for Nuclear Reactor Containment Analysis", Sandia National Laboratory, NUREG/CR-6533 (SAND97-1735), December 1997.

[12] Naumann K.–H., Bunz H.; "Computer simulations on the dynamics of fractal aerosols", *J. Aerosol Sci.* **23** (1992) S361.